CALIBRATION PROCESS AND CROSS-POL IMPROVEMENT OF AN ACTIVE X-BAND DUAL-POL PHASED-ARRAY WEATHER RADAR

Gerard Masalias-Huguet*, Krzysztof Orzel, Stephen J. Frasier
University of Massachusetts, Amherst, Massachusetts

1. INTRODUCTION

Active phased-array radars produce agile beams with shapes and sidelobe levels dictated by the phase and amplitudes of the radiating elements. The nominal settings of the array are determined through a calibration procedure, which accounts for various phases and amplitudes of the microwave components comprising the active array elements. Deviations from these nominal settings occur due to temperature, calibration setup and other environmental changes which can affect the beam properties. The stability of relative amplitudes and phases among array elements is critical to the beam quality, and hence the quality of derived weather products.

In this paper, the Phase-Tilt Weather Radar (PTWR) is used to evaluate the calibration stability through repeated measurements using different methods in the laboratory environment and near-field anechoic chamber. Open End Waveguide Probe (OEWP) and mutual coupling-based measurements were the two chosen setups to perform the calibration process. Magnitude and phase differences between methods and environments are reviewed as well as the obtained array settings in order to study their impact on the final beam forming performance.

Furthermore, in addition to the beam shape, isolation between polarizations is also critical for producing reliable polarimetric products. According to (Wang and Chandrasekar, 2006), worst case scenario requirements for Alternate Transmit Alternate Receive (ATAR) operation mode are 20 dB of isolation. Efforts to improve the Cross-Polarization Isolation Ratio (CPR) through modification of the array settings are presented, implementing a novel technique described by Sanchez et al. (2013) which allows for a cross-polarization cancellation with no additional hardware requirements. This technique will also yield better Integrated Cross-Polarization Ratio (ICPR), an essential parameter for remote sensing applications.

2. SYSTEM CALIBRATION

The system is characterized measuring the S21 parameter (see Figure 1) of each transmitter-receiver module (TRM), over different attenuator and phase shifter states, using a network analyzer. A total of 4096 states are possible in each module, however, a less time-consuming method that requires only 128 was used. The code loops through the attenuator states, while phase state is set to zero, and then loops through the phase shifter states while the attenuator is set to zero. Afterwards, a matrix containing the remaining states may be obtained using those measurements as described in (Orzel, 2014). Mode of operation, including transmit and receive, are also characterized due to the fact that they have different power requirements. TRMs work in saturation over the first 10-15 states, when using transmit mode, in order to achieve maximum range distance. Conversely, in receive mode, power is set such that highest amplitude state is not saturating the TRM gain block.

Differences over the applied methods rely on the use of external instrumentation and the number of TRMs operating simultaneously. Calibration by OEWP does require an additional instrument to measure single column radiated signals whereas mutual coupling, as the name indicates, uses self-coupling between elements

---

Corresponding author address: Gerard Masalias-Huguet, MIRSL, Univ. of Mass, 151 Holdsworthway, Amherst, MA 01003-9284;
e-mail: gerardm@umass.edu

and multiple TRMs to measure the coupled power. The signal goes through distinct paths in each method. Since mutual coupling has a closed loop, a correction to subtract part of the transmitter channel, coupling path and feeding network is needed for comparison with OEWP results.

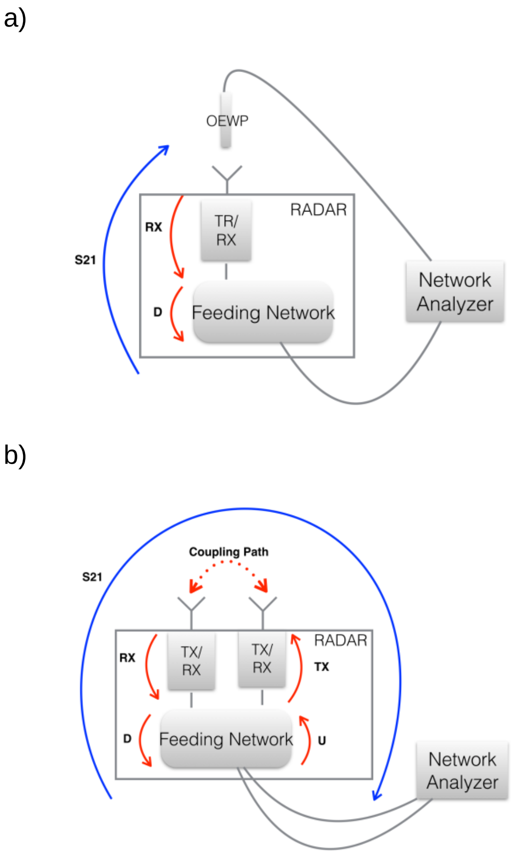

Figure 1: Calibration setups and S21 parameter paths, OWEP in a) and mutual coupling in b).

3. CROSS-POLARIZATION IMPROVEMENT

The cross-polarization cancellation technique is based on interleaved sparse arrays and is implemented for a two dimensional array in (Sanchez et al, 2013). Since PWTR is a column-fed array that scans over azimuth, a simplified version, to one degree of freedom, is briefly presented in this section.

The technique consists of dividing the array into two subsets of elements. Each subset will have its own array factor, AF_1 and AF_2. Since the antenna element is not perfect, if port 1 is excited, horizontal and vertical components of the electrical field will be radiated, f_{V1} *and* f_{H1} (idem for port 2). We set one subset in one polarization and we switch the other subset into the orthogonal polarization. We know that each field component will have contributions from both ports, thus the two components of the total electric field may be expressed as:

$$f_{TV} = AF_1 f_{V1} + AF_2 f_{V2} \tag{1}$$

$$f_{TH} = AF_1 f_{H1} + AF_2 f_{H2} \tag{2}$$

For a given direction of the main lobe, θ_0, we want to cancel one of the electric field components (the cross-polarized field, i.e. horizontal component) in order to improve the cross-polarization. Expanding the definition of array factor and taking α as the phase shift applied to each element:

$$\sum_{n=1}^{N} I_n e^{j\alpha_n} e^{jn\Psi} = -\sum_{m=1}^{M} I_m e^{j\alpha_m} e^{jm\Psi} \frac{f_{H1}(\theta_0)}{f_{H2}(\theta_0)} \tag{3}$$

For a uniformly excited array, α has to be adjusted to cancel the progressive phase shift between elements Ψ. Applying the conditions above, equation (3.3) becomes:

$$N\ f_{H2}(\theta_0) + M\ \ f_{H1}(\theta_0) = \ 0 \tag{4}$$

In summary, with N and M being the number of elements from each subset, the horizontal component of the electrical field should be theoretically canceled if the proper ratio of elements is switched co-polarization. The latter can be obtained from the measured CPR. Furthermore, both co-polar and cross-polar phases have to be measured in each polarization in order to compute the co-polarized elements phase shift needed to cancel cross-polarized field over the region of interest.

4. RESULTS

Measured S parameters from diverse calibration processes are presented along with radiation patterns measured in the near-field anechoic chamber. Afterwards, cross-polarization cancellation results are presented and discussed.

4.1 Calibration

Figure 2 shows less than 0.5 dB difference between laboratory (reflective environment) and chamber environments when OEWP was used. Since the 6-bit attenuator state has a 0.5 dB step, this distortion cannot be corrected by the system. Analogue to phase differences, in Figure 4, a 5.6 deg. step cannot correct discrepancies up to 2 deg. By contrast, mutual coupling, shown in Figures 2 and 3, presents deviations up to 1.5 dB and 10 deg., mainly due to irregularities over the antenna surface and small gaps between the antenna panels. Though far from identical, these disagreements correspond only to 2-3 states out of 64. To study the impact of these results in beamforming, an error vector was created to synthetize the radiation pattern. The latter, provided 1.4 deg. of misalignment from the main lobe center and 1 dB higher sidelobe levels.

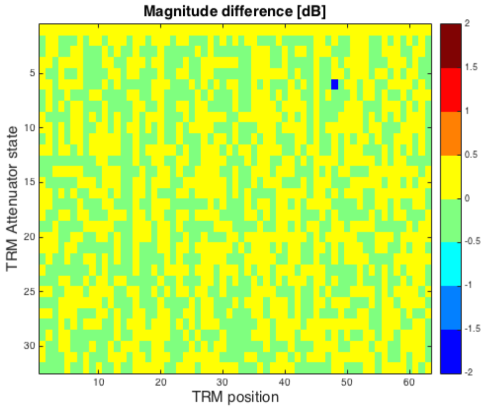

Figure 2: S21 magnitude difference in dB between anechoic chamber and laboratory environment over the first 32 attenuator states performed with OEWP.

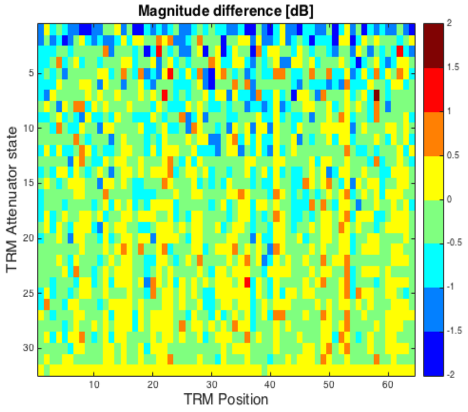

Figure 3: S21 magnitude difference in dB between mutual coupling and probe measurements conducted in laboratory environment over the first 32 attenuator states.

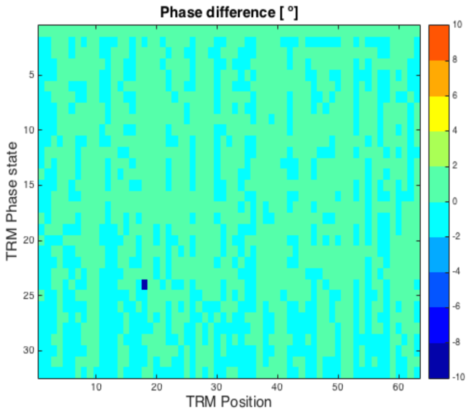

Figure 4: S21 phase difference in deg. between anechoic chamber and laboratory environment over the first 32 attenuator states performed with OEWP.

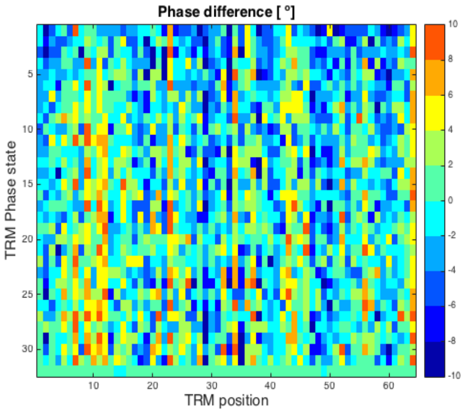

Figure 5: S21 phase difference in deg. between mutual coupling and probe measurement conducted in laboratory environment over the first 32 attenuator states.

4.2 Cross-pol cancellation

A first approach to this technique was done using 8 columns of the array. As illustrated in Figure 6, a local minimum is achieved around the area of the main lobe where the regular cross-pol had a peak. It reported more than 4 dB CPR improvement if measured at 0 deg.

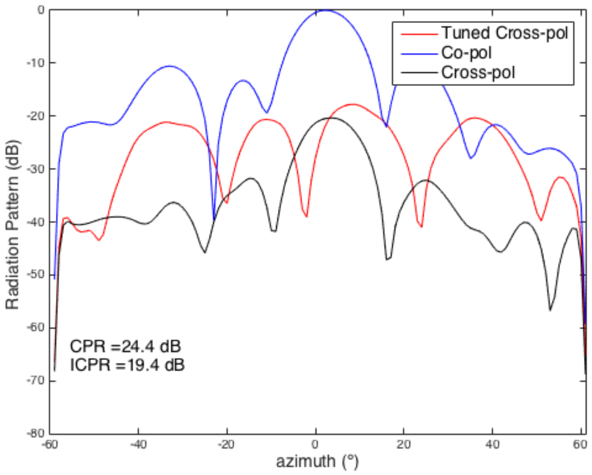

Figure 6: Co-polar and cross-polar radiation pattern for a uniformly fed 8-column array, one column switched. Improved values displayed.

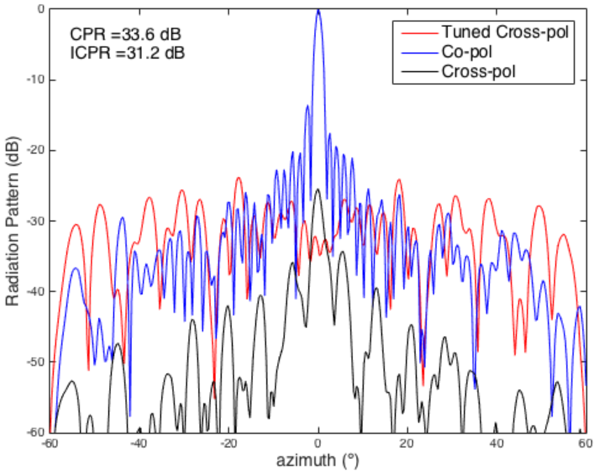

Figure 7: Full array co-polar and cross-polar radiation patterns using uniform feeding with 4 columns switched. Improved values displayed.

However, because of the early stage, tuned cross-pol is shifted a few degrees away from the broadside direction. If CPR is measured at that minimum, 17 dB of improvement was achieved. Modified settings applied to full active array, switching 4 elements into co-pol, revealed more than 8 dB improvement on CPR and 6 dB on ICPR (see Figure 7).

5. CONCLUSIONS

A calibration process with different setups has been presented, along with a cross-polarization isolation enhancement. The laboratory environment has produced successful results, with OEWP as the preferred method. However, although mutual coupling was less precise, it is still a useful technique for self-diagnostics in the field, where human access may not be realistic.

Regarding polarization isolation improvement, the technique applied to a one-dimensional scanning array appears to improve both CPR and ICPR when tested on full array. The principal drawback is higher sidelobe levels on the tuned cross-pol, due to more received power from the co-polarized elements. Effects on the co-polar pattern would be a slightly lower and wider main lobe, as fewer elements contribute to form the array factor.

6. REFERENCES

Sanchez, M., R.W. Jackson, S. Frasier, 2012: Interleaved Sparse Arrays for Polarization Control of Electronically Steered Phased Arrays for Meteorological Applications. *IEEE Transactions on Geoscience and Remote Sensing*, 50(4), 1283-1290.

Orzel, K., 2014: X-Band Dual Polarization Phased-Array Radar for Meteorological Applications. *Doctoral Dissertation from UMass Scholarworks*, 3, 41-56.

Wang, Y., and V. Chandrasekar, 2006: Polarization isolation requirements for linear dual-polarization weather radar in simultaneous transmission mode of operation. *IEEE*

Transactions on Geoscience and Remote Sensing, 44(8), 2019–2028.

This extended abstract was supported by NSF Grants AGS-0937768, AGS-1318148 to the University of Massachusetts and NSF Partnerships for Innovation - Accelerating Innovation Research Award Number 1237767 to the CASA. Any opinions, findings, conclusions, or recommendations expressed in this material are those of the authors and do not necessarily reflect those of the NSF.